Journal of Energy Bioscience 2024, Vol.15, No.1, 28-31
http://bioscipublisher.com/index.php/jeb

Scientific Commentary Open Access

Deciphering the Structural Complexity of *Populus* Secondary Cell Walls: Implications for Biomass Conversion Efficiency

Francis Burke
The BioSci Publisher, Richmond, British Columbia, Canada
Corresponding email: Francis.burke@sophiapublisher.com
Journal of Energy Bioscience, 2024, Vol.15, No.1 doi: 10.5376/jeb.2024.15.0004
Received: 05 Jan., 2024
Accepted: 08 Feb., 2024
Published: 19 Feb., 2024

Preferred citation for this article:
Burke F., 2024, Deciphering the structural complexity of *Populus* secondary cell walls: implications for biomass conversion efficiency, Journal of Energy Bioscience, 15(1): 28-31 (doi: 10.5376/jeb.2024.15.0004)

The paper titled "Atomistic, macromolecular model of the *Populus* secondary cell wall informed by solid-state NMR" was published on January 3, 2024, in the open-access journal Science Advances, under the Science Publishing Group. The authors, Bennett Addison, Lintao Bu, Vivek Bharadwaj, Meagan F. Crowley, Anne E. Harman-Ware, Michael F. Crowley, Yannick J. Bomble, and Peter N. Ciesielski are from National Renewable Energy Laboratory and the Colorado School of Mines in Golden, CO, USA. The study presents an atomistic macromolecular model of the secondary cell wall (SCW) in *Populus* wood, focusing on the interactions and configurations of cellulose, hemicelluloses, and lignin. Utilizing solid-state nuclear magnetic resonance (ssNMR) measurements, the research investigates the structural configurations and intermolecular interactions within the SCW. This information is used to develop and refine molecular models through molecular dynamics (MD) simulations, enhancing the understanding of the SCW's architecture and informing biomass deconstruction strategies.

1 Interpretation of Experimental Data

The research highlight the spatial arrangement and interactions of cellulose, xylan, and lignin within the SCW. The 1D 1H-13C MultiCP-MAS ssNMR spectrum identifies distinct environments for cellulose and indicates the presence of acetylated xylan and lignin. Selective 1D MultiCP-DARR difference data quantify polymer-polymer contacts at the nanometer scale, showing how magnetization moves between carbon environments, providing crucial distance information for constructing accurate molecular models.

Figure 1 presents a comprehensive analysis of lignified *Populus* secondary cell walls (SCWs) using 1D 1H-13C MultiCP-MAS solid-state NMR (ssNMR). The spectrum delineates the chemical environments of the primary polymers: cellulose (gray), xylan (blue), and lignin (green), with specific regions assigned to their characteristic peaks. Cellulose's assignments include peaks for C1, C2, C3, C5, and C6 carbons. Xylan is highlighted by signals corresponding to acetylation and glucuronic acid residues. Lignin's spectrum reveals syringyl (S) and guaiacyl (G) units, identified through their aromatic and side-chain carbons, including the notable β-O-4 linkages. The black trace represents the raw data, while the red trace shows the fitted model, illustrating the accuracy of the spectral deconvolution informed by the combined 1D and 2D ssNMR data. This detailed spectral analysis aids in understanding the complex structural composition and interactions within *Populus* SCWs.

Figure 3 illustrates atomistic models of *Populus* secondary cell walls (SCWs) with various arrangements of cellulose, xylan, and lignin. The left panel shows several model variants, named based on the arrangement of hemicellulose and lignin. For instance, model "a" has all xylan bound to cellulose, while "b" models have 70% xylan bound to cellulose and 30% interspersed with lignin. The right panel presents a polar plot comparing the percentage of sink atoms within 1 nm of source atoms in these models against experimental ssNMR spin-diffusion data. The models vary in their alignment with experimental data, indicating different structural proximities within SCWs.

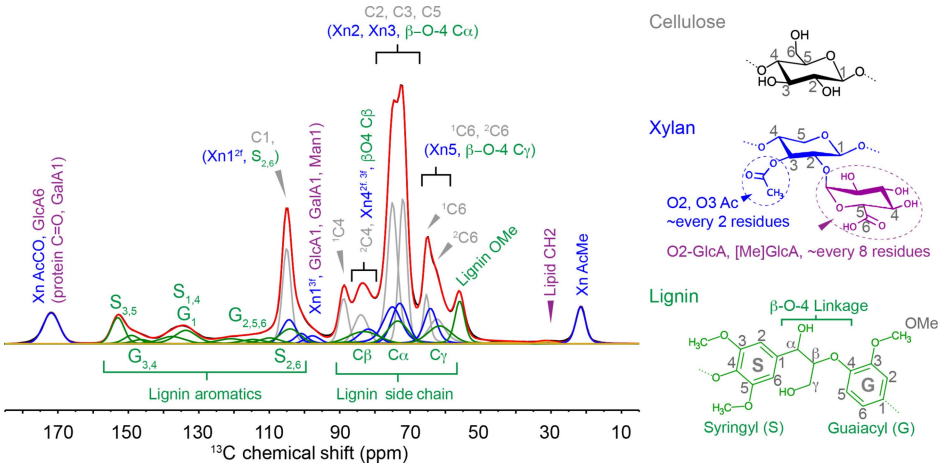

Figure 1 1D ^{1}H-^{13}C MultiCP-MAS ssNMR provides a broad overview of lignifed *Populus* SCWs

Note: General assignment regions are indicated for the predominant constituent polymers cellulose (gray), xylan (blue), and lignin (green), along with representative structures and their assignments indicated with color-coding. chemical shift information and peak profles extracted from a combined set of 1d and 2d ssnMR data were used to inform spectral deconvolution efforts used throughout this work; The raw data are shown in black, and the resultant ft is shown in red; c: Cellulose; Xn: Xylan; Ac: Acetyl; GalA: Galacturonic acid (pectin); GlcA: α-d-glucuronic acid; [4OMe] GlcA: (4-O-methyl)-α-d-glucuronic acid

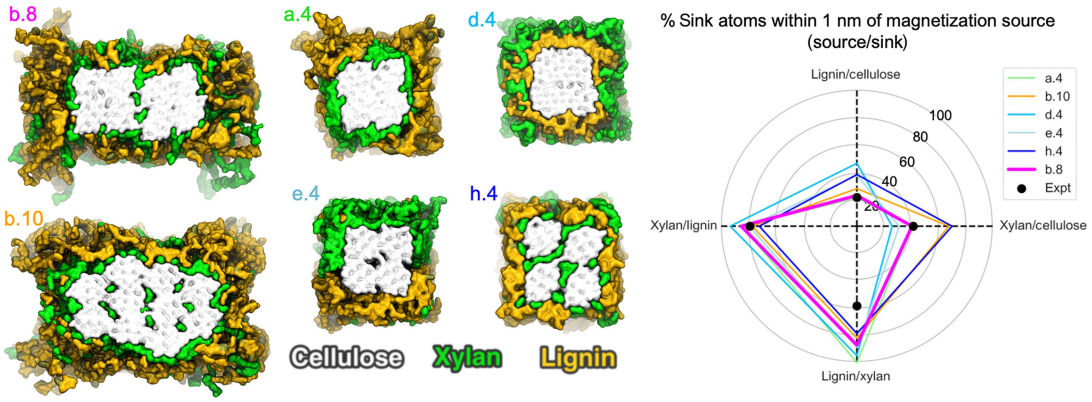

Figure 3 Atomistic SCW periodic model variants and comparison of their proximity analyses with ssNMR spin-diffusion experiments

Note: Left: Snapshots of several molecular model variants for the poplar ScW. the naming convention is as follows: the letter refers to the relative arrangement of hemicellulose and lignin, where “a” denotes a model with all xylan bound on cellulose, and no xylan interspersed with lignin; “b” denotes a model with 70% hemicellulose bound to cellulose, and the remaining 30% interspersed in the surrounding lignin-xylan matrix; “d” denotes a model with lignin-bound cellulose and with hemicellulose as the surrounding layer; “e” denotes a model with phase-separated hemicellulose and lignin both bound to cellulose at the top and bottom, respectively; “h” denotes a model with hemicellulose interspersed within the 18-chain elementary cellulose fbril leaving room for increased direct lignin-cellulose interaction. the number after the decimal denotes the number of 18-chain elementary fbrils in the model. b.8 and b.10 are larger systems constructed with 70% of xylan bound to cellulose, and the remaining 30% interspersed with lignin and consist of eight and ten 18-chain cellulose elementary fbrils, respectively; Right: Calculated percentage of sink atoms within 1 nm of source atoms in the model variants compared to that obtained from ssnMR spin-diffusion experiments depicted on a polar plot; The four dashed lines originating from the center indicate the four ssnMR magnetization metrics, with the experimental values indicated as black dots and the colors indicating the various models

Figure 4 depicts the atomistic model of lignocellulose assembly within *Populus* secondary cell walls (SCWs), aligning with ssNMR data. Panel A shows the molecular structures of lignin, xylan, and cellulose. Panel B illustrates their macromolecular assembly, where xylan on the cellulose surface adopts an extended configuration, pointing towards lignin. Panel C highlights the cellulose component, comprising two core bundles of four 18-chain elementary fibrils. Panel D focuses on hemicellulose, revealing a nearly complete sheath around cellulose, minimizing direct cellulose-lignin contact and some xylan isolated within core bundles. Panel E indicates that lignin primarily interacts with hemicellulose, with minimal direct contact with cellulose. This model underscores the spatial organization and interactions of these biopolymers, crucial for SCW integrity.

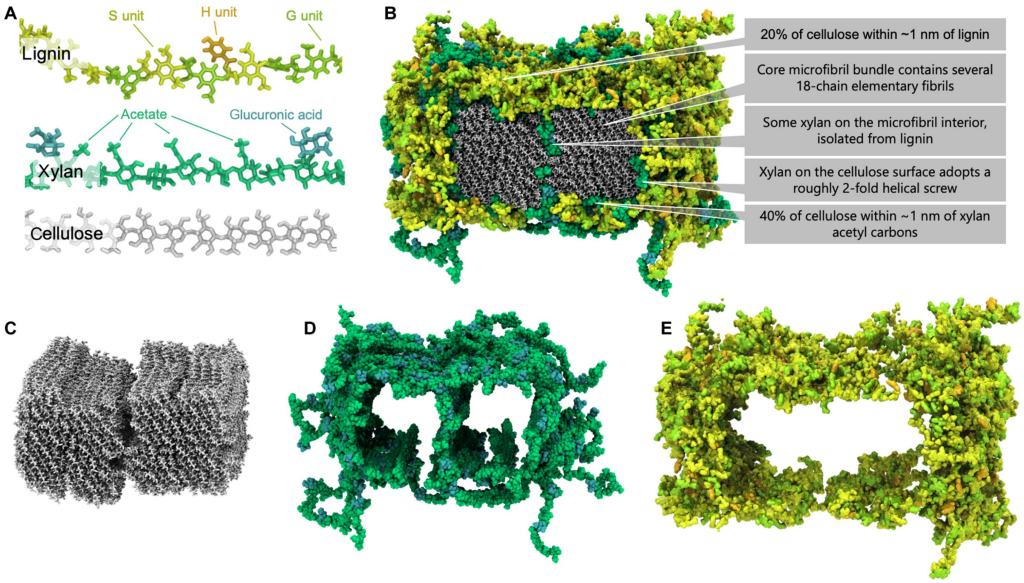

Figure 4 Atomistic model of the lignocellulose assembly within the *Populus* SCW that best represents ssNMR observables
Note: (A) Molecular representation of the individual biopolymer constituents. (B) Macromolecular assembly of cellulose, xylan, and lignin. the xylan domains on the surface of cellulose adopt an extended confguration with decorations pointing away from the cellulose surface toward lignin. (C) visualization of the cellulosic components only, showing two core bundles comprising four 18-chain elementary fbrils. (D) visualization of the hemicellulose components only shows the nearly complete sheath formed around the cellulose minimizing direct contact between cellulose and lignin; also, some xylan is found between core bundles, isolated from lignin. (E) lignin interacts predominantly with hemicellulose and displays minimal direct contact with cellulose

Figure 5 contrasts the conformations of xylan polymers based on their proximity to cellulose. Panel A shows that xylan bound to cellulose adopts conformations with acetate groups consistently oriented away from the surface, while unbound xylan displays random acetate group orientations. Panel B highlights the broad distribution of φ + ψ dihedral angles in unbound xylan, peaking around 170°. Panel C indicates that bound xylan, despite a wide φ + ψ distribution, prominently peaks at approximately 100°. Panel D demonstrates a wide θ2f (O2-C5-C5-O2) dihedral angle distribution for unbound xylan, reflecting nonuniform acetate orientations. Conversely, Panel E shows a narrow θ2f distribution centered at 0° for bound xylan, signifying consistent acetate orientations. Panels F and G define these dihedral measurements, emphasizing structural differences driven by cellulose binding.

2 Insight of Research Findings

The study shows that the SCW's mechanical integrity and resistance to deconstruction arise from the complex interactions between cellulose, hemicelluloses, and lignin. The ssNMR data reveal subnanometer interactions, essential for understanding the SCW's structure. Molecular dynamics simulations support these findings, confirming the significance of initial polymer placement and suggesting minimal rearrangement over time.

3 Evaluation of the Research

The research successfully integrates ssNMR data with molecular dynamics simulations to provide a detailed macromolecular model of the SCW. The study's approach offers valuable insights into the structural arrangement of biopolymers, contributing to a better understanding of lignocellulosic biomass and its potential applications. However, limitations include the reliance on spectral deconvolution and the need for further investigation into different cell types and more mature wood samples.

4 Concluding Remarks

The study advances our understanding of the SCW architecture in *Populus* wood, highlighting the importance of polymer interactions at the nanometer scale. The integration of experimental and computational methods provides a robust framework for future research on plant cell wall structures and their applications in renewable energy and materials science.

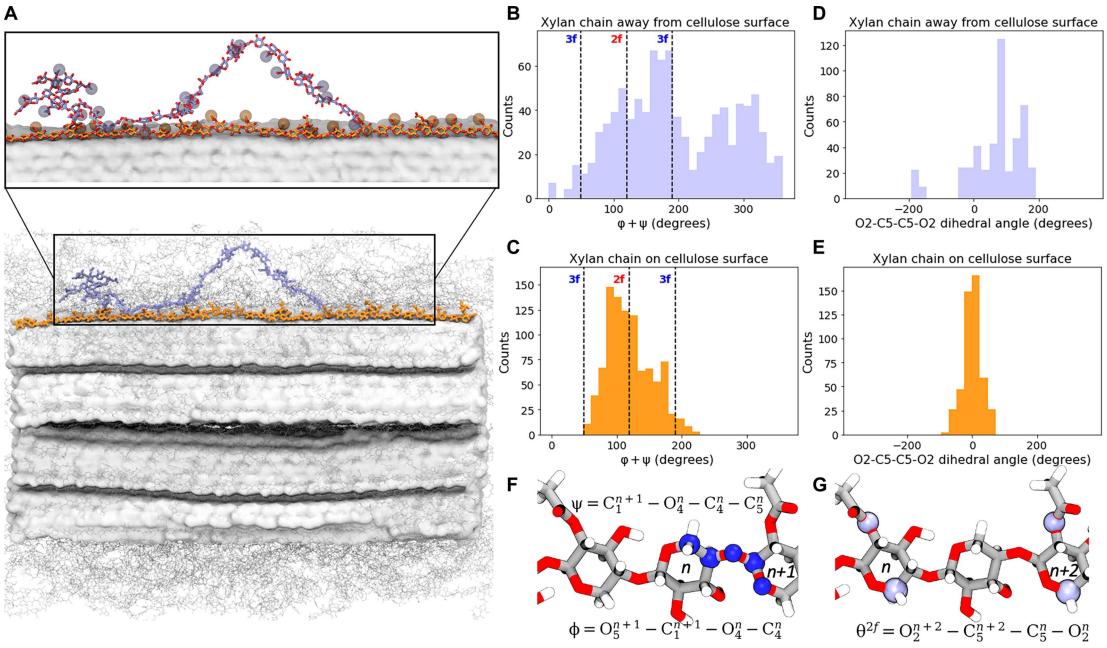

Figure 5 Contrasting conformation of xylan polymers with different proximities to cellulose

Note: (A) Xylan bound to cellulose (orange) adopts conformations that enable acetate groups to consistently orient away from the cellulose surface. Unbound xylose (light blue) adopts a more random orientation of acetate groups. exemplary xylan polymers are shown in licorice representation, with their acetate groups highlighted as spheres, and cellulose is shown as a white surface. (B) Unbound xylan φ + ψ distributions are not exclusively 31 and span a large range of values with a peak at ~1700. (C) For xylan chains with similarly oriented acetate groups, a wide distribution of canonical φ + ψ conformations is observed, although a peak ~1000 is prominent. (D) θ2f(O2-c5-c5-O2) values for the unbound xylan chain are widely distributed corresponding with the nonuniform acetate group orientations. (E) Bound xylan exhibits a narrow θ2f distribution centered at 00, which highlights the consistent orientation of acetate groups. defnition of canonical φ + ψ and θ2f(O2-c5-c5-O2) dihedral measurements is portrayed in (F) and (G), respectively

5 Access the Full Text

Addison B., Bu L.T., Bharadwaj V., Crowley M.F., Harman-Ware A.E., Crowley M.F., Bomble Y.J., and Ciesielski P.N., 2024, Atomistic, macromolecular model of the *Populus* secondary cell wall informed by solid-state NMR, Science Advances, 10(1): eadi7965. https://www.science.org/doi/full/10.1126/sciadv.adi7965

Acknowledgement

I sincerely appreciate the open-access policy of Science Advances, which allows readers to freely share this valuable research. I would also like to thank the research team led by Yannick J. Bomble, and Peter N. Ciesielski for their outstanding work, which provides a valuable case for studies on plant cell wall architecture and its implications for renewable energy and materials science. Given that reviewers may have different perspectives on the interpretation of the data and results, I apologize if my analysis and evaluation differ from the authors' original intent. I look forward to further research to delve deeper into the complexities of this field.